

# Towards Explaining Anomalously Large Body Voltage Surges on Exceptional Subjects Part I: The Electrostatic Approximation

WILLIAM A. TILLER

*Dept. of Materials Science and Engineering, Stanford University, Stanford, CA 94305-2205*

ELMER E. GREEN, PETER A. PARKS, AND STACY ANDERSON

*Center for Applied Psychophysiology, The Menninger Clinic, 5800 W. 6th Ave., Topeka, KS 66606*

**Abstract** — A simple electric dipole model, in the static limit, was used to analyze simultaneous voltage recordings from the ear of an experienced non-contact therapeutic touch specialist and from four surrounding copper walls during a 30-minute therapy session wherein 15 ear voltage surges were recorded, ranging between  $-20$  V and  $-80$  V from baseline with time durations from approximately 0.5 to 12.5 s. In 13 of these 15 voltage surges, the origin of the dipole was located in the abdominal region and the dipole length extended from the ear to the feet with the ear always negative. In the other 2 cases a second dipole may also form in the head. A possible mechanism is given for the formation of these electric dipoles.

## Introduction

In a recent paper, Green *et al.* (1991) reported on their findings in a copper-wall laboratory experiment with 9 "exceptional" subjects, experienced therapeutic touch (TT) (Krieger, 1995) therapists: 6 women and 3 men. During TT sessions with patients, these therapists produced large anomalous body-potential surges (measured at an ear lobe) ranging from  $-4$  V to  $-190$  V, lasting from approximately 0.5 s to 12.5 s, measured with an electrometer having an input impedance of  $10^{14}$  ohms. On average, these electrical signals were approximately  $10^3$  times larger than psychophysiological galvanic skin-potential (GSP) changes associated with emotional responses,  $10^5$  times larger than electrocardiographic (EKG) voltages, and  $10^6$  times larger than electroencephalographic (EEG) voltages.

On the surrounding four copper walls, voltage signals were recorded in synchrony with the therapist's surge of body potential. Thus, for each body-potential surge, five independently measured time-varying voltages are available in the data record:  $V_b$ ,  $V_F$ ,  $V_B$ ,  $V_U$ , and  $V_D$ , where subscripts b, F, B, U and D refer to body, front wall, back wall, up (top) wall and down (bottom) wall, respectively. This accumulation of electrical data is sufficiently rich that modeling of its origins seems possible.

The purpose of this paper is to set forth a working hypothesis concerning the origins of these anomalous voltage surges and to explore theoretically the

model in terms of its electrostatic asymptotic limit. Match between theory and experiment is made in the electrostatic limit where only the maximum *amplitude* of the voltage signals is utilized in order to gain an overall picture of what is occurring. In a subsequent paper, the more complex *electrodynamic* aspects of the model will be considered (time dependence and detailed shape of the voltage). Here, in an analysis of data generated by a *single* therapist in one 30-minute TT session (Subject 70, Session 7, wherein 15 anomalous body-potential surges were recorded) we shall see the growth and collapse of an electric dipole in the lower abdominal region. This dipole, with modest charge displacement, is sufficient to accommodate most of the experimental findings. Session 7, incidentally, was the *first* TT session of Subject 70 (Green *et al.*, 1991). In 15 subsequent sessions, 92 similar anomalous body-potential surges were generated.

### Qualitative Summary

It appears from the data of Green *et al.* that the training and practice involved in TT develops in the healer a somewhat automatic internal power buildup at subtle levels of the body that discharges periodically and generates a very large electrical voltage pulse in the physical body. This voltage pulse is measured both via an ear electrode and via nearby very large copper-wall electrodes. When the healer is intentionally healing, these internal voltage surges increase in both frequency and magnitude. The subject studied here generated 15 anomalous surges during one 30-minute healing session.

The theoretical model proposed to account for this remarkable voltage phenomenon is a transduced field effect which starts from an hypothesized level of subtle substance in the healer's body and ends at a measurable level of electrical substance in the healer's body. The underlying physical signal is thought to be a magnetic vector potential pulse. From conventional electro-dynamics, such a pulse always generates a bipolar electric field pulse in the immediate vicinity of the source. This, in turn, acts on nearby electrolytes of the physical body to generate first an expanding and then a collapsing electric dipole in the physical body. It is this electric dipole that gives rise to voltage signals in the healer's body and on the copper walls. These voltages are the readily detectable correlates of the original subtle energy pulse which is hypothetically associated with the intention to heal.

Using this conceptual model, a mathematical model has been developed for this electric dipole generation. This model predicts the voltage at any body or remote location and has been found to predict (1) the origin of the dipole in the physical body, (2) the amount of electric charge involved in forming the dipole and (3) the distance over which the charge must be transferred to create this dipole.

For the first time, it is possible to treat what we normally consider to be an elusive and statistically marginal phenomenon in a robust and pragmatic way, finding that the data stand up well to such quantitative scrutiny. The clear

agreement between non-statistical theory and experiment lends support to the hypothesis of subtle physical substance and its ability to interact with traditional physical substance to produce an hypothesized magnetic vector potential.

### Theoretical Modelling

A. *Working Hypotheses:* (1) It is proposed that each voltage surge is a convolution of several gaussian-type sub-pulses. The detailed shape of sub-pulses is not known, but a gaussian shape will serve as a first approximation. (2) Further, it is also proposed that a single gaussian-type sub-pulse is associated with the time-dependent growth and collapse of a single electric dipole located in the body. (3) The time-dependent charge separation associated with the dipole is thought to be the source for  $V_b$ ,  $V_F$ ,  $V_B$ ,  $V_U$  and  $V_D$ . (4) The maximum charge dipole at the point of maximum charge separation correlates with the maximum of a gaussian sub-pulse and constitutes the electrostatic limit approximation invoked in this paper.

B. *Charge Dipole Electrostatics from a Single Source:* The geometrical configuration of the copper wall room is presented in Fig. 1. For this TT study, the magnet (M) was removed. The relevant geometry and distances for the proposed dipole are given in Fig. 2 where:

$$X_F - X_B = L = 85.5"; Y_U - Y_D = L = 85.5"; \quad (1)$$

$$Y_U - Y_E = Y*; X_F - X_E = X*$$

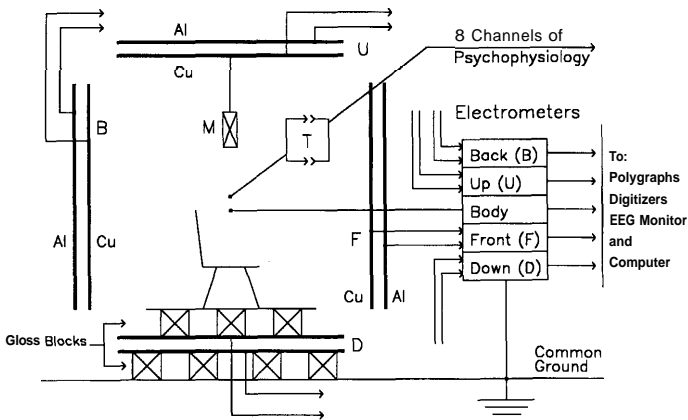


Fig. 1. Schematic diagram of copper-wall meditation room. Four pairs of insulated copper (Cu) and aluminum (Al) panels float in electrical space around a research chair which also floats electrically, insulated from the down wall (D) by glass construction blocks. A bar magnet (M) is suspended over the subject's head during meditation and 8 battery-powered channels of psychophysiological data lead to the control room via optical telemetering (T). Signals from the four Cu panels, front (F), back (B), up (U), down (D), and from the subject's body, are fed into single-ended electrometers. Al panels reach common ground through their electrometers. Data from all channels are forwarded to polygraphs, digitizers, and a computer. Two video cameras that watch subjects during sessions (one on each side) are not shown.

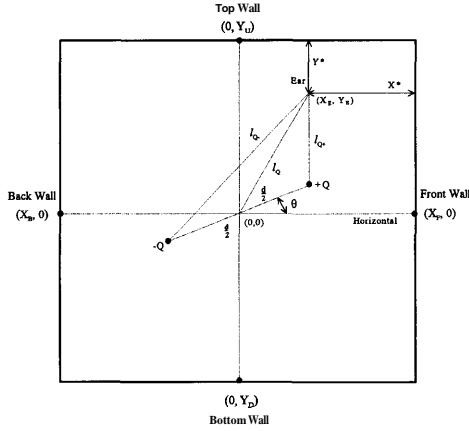


Fig. 2. Geometrical arrangement of electric dipole relative to the ear and the four copper walls.  $Y^*$  and  $X^*$  are the distances from the subjects' ear to the top wall and to the front wall, respectively. Charge  $Q$  is shown as a dipole with plus and minus components,  $+Q$  and  $-Q$ , separated by a distance  $d$ .  $l$  is the distance from the center of the dipole, at origin  $(0,0)$ , and  $l_{q+}$  and  $l_{q-}$  are the distances from the ear to the  $+$  and  $-$  charges.

Subscript E refers to the subject's earlobe, where the body-potential electrode is attached. We are interested in determining the coordinates of the dipole's origin relative to the front and down walls, and the angle of inclination,  $\theta$ , for separation of charge  $Q$  over a distance  $d$ . Since we have 5 unknowns and 5 independent pieces of information (five measured voltages), we should be able to solve for the unknowns provided we know  $(X^*, Y^*)$ . This  $(X^*, Y^*)$  data for the 15 voltage surges to be investigated is given in Table 1. To simplify analysis, we shall initially neglect (1) multiple-charge image effects in the walls, (2) opposite-sign ion condensation from the air onto the walls and (3) any internal dielectric characteristics of the body.

TABLE I

Time From 0:00	Distance From:			
	Front Wall	Back Wall	Up Wall	Down Wall
3:20	61"	24 1/2"	27 1/4"	58 1/4"
3:30	61"	24 1/2"	27 1/4"	58 1/4"
3:57	61"	24 1/2"	27 1/4"	58 1/4"
5:48	61"	24 1/2"	27 1/4"	58 1/4"
15:49	43 1/2"	42"	25"	60 1/2"
16:54	43 1/2"	42"	25"	60 1/2"
17:18.5	43"	42 1/2"	25"	60 1/2"
19:48.5	43"	42 1/2"	25"	60 1/2"
22:33	41 1/2"	44"	26"	59 1/2"
23:46	42 1/2"	43"	25"	60 1/2"
25:00	47"	38 1/2"	29"	56 1/2"
26:59	44"	41 1/2"	25 1/2"	60"
27:27	46 1/2"	39"	28"	57 1/2"
27:35	46"	39 1/2"	28"	57 1/2"
27:54	47 1/2"	38"	31"	54 1/2"

Approximate location of right ear during  $V_b$  surges for Subject 70, Session #7

It is well known that the voltage  $V$  developed at distance  $r$  from a charge  $Q$  is given by the simple formula (Kraus, 1973) :

$$V = Q/4\pi\epsilon r \tag{2a}$$

Where  $\epsilon$  is the permittivity of the medium ( $\epsilon = 10^{-9}/36\pi$  farads per meter for air or vacuum). To incorporate the effects of multiple images, ion condensation and dielectric response, we can modify Equation 2a to the form:

$$V = \alpha Q/4\pi\epsilon\epsilon' r \tag{2b}$$

Where  $\alpha = \alpha_1\alpha_2$ ;  $a, \geq 1$  incorporates the multiple image contribution while  $\alpha_2 \leq 1$  incorporates the opposite-sign ion condensation. In addition,  $\epsilon' \geq 1$  and is a function of location and time and incorporates the body internal dielectric-response effects. As previously mentioned, for the majority of this paper, we shall use the simplifying approximation,  $a = \epsilon' = 1$ .

In evaluating the electrostatic limit for the wall and body voltages, one often invokes the  $d/l_Q \ll 1$  approximation where, in this case,  $l_Q$  is the distance from the ear to the origin (0, 0) of the dipole. Using Equation 2a with this approximation we have:

$$V_f = \frac{Q}{4\pi\epsilon} \left[ \frac{1}{X_F - \frac{d}{2} \cos \theta} - \frac{1}{X_F + \frac{d}{2} \cos \theta} \right] \approx \frac{Q}{4\pi\epsilon} \frac{d \cos \theta}{X_F^2} \tag{3a}$$

$$V_b = \frac{-Q}{4\pi\epsilon} \frac{d \cos \theta}{X_B^2}, \tag{3b}$$

which yields

$$\frac{V_F}{V_B} = - \left( \frac{X_B}{X_F} \right)^2, \tag{3c}$$

so that

$$X_F = \frac{L}{\left[ 1 + \left( -\frac{V_F}{V_B} \right)^{1/2} \right]} \tag{3d}$$

In a similar fashion, we find that

$$V_U = \frac{Q}{4\pi\epsilon} \frac{d \sin \theta}{Y_U^2} \quad (4a)$$

$$V_D \approx \frac{-Q}{4\pi\epsilon} \frac{d \sin \theta}{Y_D^2}, \quad (4b)$$

and

$$V_D = \frac{L}{\left[1 + \left(-\frac{V_D}{V_U}\right)^{1/2}\right]} \quad (4c)$$

Thus, by utilizing the ratios of the opposing wall voltages, the position of the dipole source (0, 0) can be found relative to the front and bottom walls ( $X_F, Y_D$ ). When we make the following definitions,

$$\begin{aligned} \Delta V_1 &= V_F + V_B \\ \Delta V_2 &= V_U = V_D \end{aligned} \quad (5a)$$

we can use Eqs. 3 and 4 to yield

$$\frac{Qd}{4\pi\epsilon} = \frac{\Delta V_1}{\cos \theta \left[ \frac{1}{X_F^2} - \frac{1}{(L - X_F)^2} \right]} \quad (5b)$$

and

$$\tan \theta = \frac{\Delta V_2}{\Delta V_1} \left[ \frac{\frac{1}{X_F^2} - \frac{1}{(L - X_F)^2}}{\frac{1}{Y_U^2} - \frac{1}{(L - Y_U)^2}} \right] \quad (5c)$$

Thus, both the angle  $\theta$  and the  $Qd$  product can also be determined from a knowledge of the wall voltages.

To obtain a value for  $d$  or  $Q$  separately, we must use our final piece of information,  $V_b$ , measured at the subject's ear and given by

$$V_b = \frac{Q}{4\pi\epsilon} \left[ \frac{1}{l_{Q+}} - \frac{1}{l_{Q-}} \right] \quad (6a)$$

Expressing  $l_{Q+}$  and  $l_{Q-}$  in trigonometric terms from Fig. 2 and utilizing Eq. 5, Eq. 6a yields

$$d = \frac{\Delta V_1}{V_b} \left[ \frac{1}{\cos \theta \left\{ \frac{1}{X_F^2} - \frac{1}{(L - X_F)^2} \right\}} \right] \times F \quad (6b)$$

where

$$F = \left[ \frac{1}{\left\{ \left( X_E - \frac{d}{2} \cos \theta \right)^2 + \left( Y_E - \frac{d}{2} \sin \theta \right)^2 \right\}^{1/2}} - \frac{1}{\left\{ \left( X_E + \frac{d}{2} \cos \theta \right)^2 + \left( Y_E + \frac{d}{2} \sin \theta \right)^2 \right\}^{1/2}} \right] \quad (6c)$$

Before attempting to match these equations with the physical data, let us note that, in the equations needed in the limit,  $d/X_F$  is not small (thus,  $d/l_Q \geq 1$ ). These are :

$$V_F = \frac{Q}{4\pi\epsilon} \left[ \frac{1}{X_F + Y_E \cot \theta} - \frac{1}{X_F - Y_E \cot \theta} \right] \quad (7a)$$

$$V_B = \frac{-Q}{4\pi\epsilon} \left[ \frac{1}{L - X_F + Y_E \cot \theta} - \frac{1}{L - X_F - Y_E \cot \theta} \right] \quad (7b)$$

$$V_D = \frac{-Q}{4\pi\epsilon} \left[ \frac{1}{L - Y_U + Y_E} - \frac{1}{L - Y_U - Y_E} \right] \quad (7c)$$

$$V_D = \frac{Q}{4\pi\epsilon} \left[ \frac{1}{L - Y_U + Y_E} - \frac{1}{L - Y_U - Y_E} \right] \quad (7d)$$

and

$$V_b = \frac{Q}{4\pi\epsilon} F \quad (7e)$$

### Fitting Theory to the Experimental Data

This section deals with the curve-fitting exercise to estimate the magnitude of the dipole-model parameters from the experimental data. The raw data for

one of the 15 anomalous events investigated is the pulse centered at time  $t = 3:20$  minutes of Fig. 3. During this body-potential surge the therapist was seated on a stool and was facing north (facing the front wall). This pulse may be treated as a convolution of several Gaussian-type sub-pulses and, using a deconvolution program', Fig. 4 shows the sub-pulses for  $V_b$ . The numerical details (center time in seconds, widths in seconds and height in volts) for this pulse are given in Table 2 for  $V_b$ ,  $V_F$ ,  $V_B$ ,  $V_U$  and  $V_D$ . Similar type data, plus orientation of the therapist (see Table 3), was available for each of the fifteen events investigated. Our assumption is that, although each anomalous event is

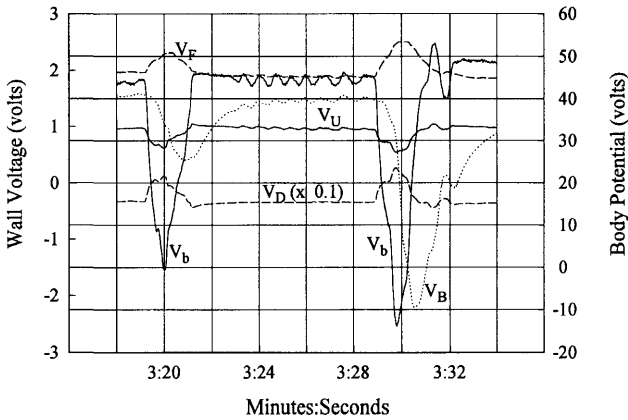


Fig. 3. Simultaneous body and wall potentials for the anomalous voltage bursts at 3:20 and 3:30 (Subject 70, Session 7).

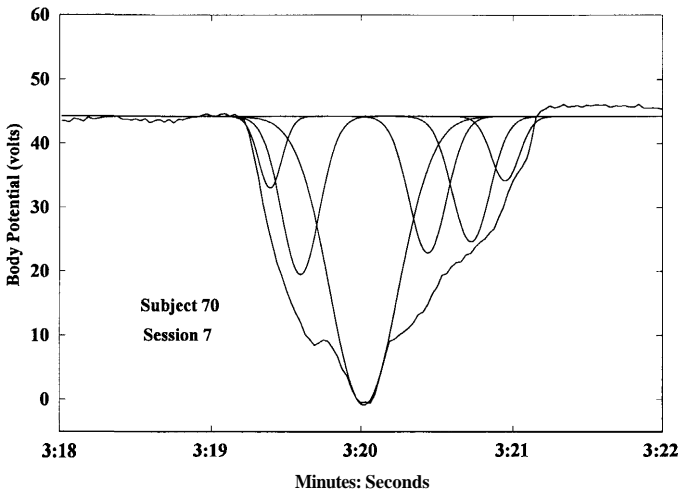


Fig. 4. Deconvolution gaussian sub-pulses for the body-potential surge at  $t = 3:20$  of Figure 3.

'Deconvolution of surges was obtained with a SpectraCalc software program marketed by Galactic Industries, modified to allow visual best-fit of gaussian curves.

TABLE 2

	Time(s) Center	Volts Height	Time(s) Width
Front Wall Baseline = 2.0 V	3:20.3	0.30	0.66
	3:20.8	0.08	0.32
	3:19.6	0.15	0.52
	3:19.0	0.06	0.25
Back Wall Baseline = 1.5 V	3:20.9	-1.08	1.69
	3:20.3	-0.22	0.39
	3:19.9	-0.16	0.25
Up Wall Baseline = 1.0 V	3:20.8	-0.10	0.34
	3:20.3	-0.17	0.39
	3:20.0	-0.36	0.49
	3:19.6	-0.04	0.14
	3:19.4	-0.23	0.43
Down Wall Baseline = -3.2 V	3:20.8	0.96	0.30
	3:20.3	2.13	0.36
	3:20.0	4.48	0.48
	3:19.6	0.68	0.17
	3:19.5	2.78	0.27
	3:19.3	1.35	0.14
Body Potential Baseline = 44.1 V	3:20.9	-8.64	0.26
	3:20.6	-19.90	0.45
	3:20.3	-6.02	0.23
	3:20.0	-44.41	0.64
	3:19.5	-19.34	0.34
	3:19.3	-4.10	0.16

Deconvolution data for the 3:20 pulse. (Subject 70, Session 7, Time = 3:20)

TABLE 3

Time (From 0:00)	Subject Orientation (North = 0°)	Comments
3:20.0	0°	Subject sitting on stool. No body motion detected.
3:30.0	0°	Subject sitting on stool. No body motion detected.
3:57.0	0°	Circular hand motion present between surges at 3:20 and 3:30. Subject sitting on stool. Very slight head motion ending just prior to surge.
15:49.0	315°	Subject standing. No body motion detected.
16:54.5	315°	Subject standing. Very slight head movement.
17:20.5	315°	Subject standing. Slight head and body motion.
19:48.5	270°	Subject standing. No body motion detected.
22:30.0	270°	Subject standing. Slight head and body motion.
23:46.0	315°	Subject standing. No body motion detected.
25:00.0	315°	Subject standing. Slight head and body motion.
26:59.0	337°	Subject standing. Slight head and body motion.
27:25.0	315°	Subject standing. No body motion detected.
27:35.0	337°	Subject standing. No body motion detected prior to 27:36. Movement of hands occurred after this time.
27:50.0	315°	Subject standing in stooped position. Small head and body motions.

Orientation and body-position of Subject 70 during 15 body-potential surges of Session 7

not a single dipole event, each gaussian curve in the deconvolution pattern is a single dipole event and is thus suitable for matching with the theory. Thus, in the electrostatic limit, it is only the height of the gaussian-type pulse that is relevant in the analysis.

As a first test, let us consider the three largest gaussian-type subpulses of Table 2 and apply Eqs. 3d, 4c, 5b and 5c to determine  $X_F$ ,  $Y_U$  for each of these sub-pulses. Finally, this data is inserted into Eq. 6c to gain separate values for  $Q$  and  $d$ . In this way, we can develop some initial insights into this dipole development and also see if the  $d/l \ll 1$  approximation holds.

The results of this analysis for the three selected gaussians are presented in Table 4. There, we see that the origin for all three pulses is essentially the same; i.e., in the lower abdomen and tilted downward at an angle  $\theta = -70^\circ$  to the horizontal. Since the subject is sitting on a stool, this would be approximately on a line between the ears and the feet. However, looking at the last column of Table 4, we see that  $d$  equals approximately 59 inches for all three cases which violates our initial assumption that  $d/l \ll 1$ . This means that, although the qualitative conclusions of Table 4 are probably correct, the quantitative results are probably in error.

TABLE 4

Time From 0:00	$V_b$ volts	$V_F$ volts	$V_B$ volts	$V_U$ volts	$V_D$ volts	$X_F$ inches	$Y_D$ inches	$\theta$ deg	$Qd$ charge-in	$d$ in
3:19.5	-19.34	0.06	-0.16	-0.23	2.13	53	18.9	-77	$0.54 \times 10^{-10}$	~59
3:19.9	-44.41	0.3	-1.07	-0.36	4.48	56	18.9	-60	$1.3 \times 10^{-10}$	~59
3:20.6	-19.9	0.15	-0.22	-0.17	2.78	47	18.9	-72	$0.78 \times 10^{-10}$	~59

Analysis of three sub-pulses for one body-potential surge (Subject 70, Session 7, Time 3:20)

The tentative conclusions to be made from the results of Table 4 are:

- 1) the dipole origin is in the lower abdomen region.
- 2) the charge separation extends from the head to the feet.
- 3) all of the gaussian surges in a single pulse have the same origin, and
- 4) the charge separation is such that the feet are positive while the ear is negative.

As a second test, let us consider only the central gaussian of the fifteen pulses under consideration and use Eqs. 7 to evaluate  $X_F$ ,  $Y_D$ ,  $\theta$ ,  $Q$  and  $d$ . The amplitudes of these gaussians are listed in Table 5. We note that:

- 1)  $V_b$  is always in the negative direction,
- 2)  $V_D$  is always in the positive direction and,
- 3)  $V_F$ ,  $V_B$ , and  $V_U$  do not show a completely consistent positive or negative pattern.

From our first test, if the origin of the dipole is in the lower abdomen, we can make the assumption that  $X_F \ll Y_E$ . Then, noting that  $V_b < 0$  while  $Q > 0$ , Eq.

TABLE 5

Time From 0:00	$V_D$	$V_U$	$V_F$	$V_B$	$V_b$	$Y^*$	$\beta$	$\gamma$	$(\beta+1)/\gamma$	$a$	$b/Y^*$	$Y_{U1}$	$Y_{U2}$
3:20	4.48	-0.36	0.29	-1.07	-44.40	27.25	-12.50	-0.46	25.00	82.50	55.80	54.10	28.40
3:30	6.10	-0.42	0.67	-3.67	-57.80	27.25	-14.50	-0.88	24.60	82.30	55.70	52.60	29.80
3:57	8.28	-0.56	0.72	-4.20	-79.60	27.25	14.80	-0.56	24.60	82.30	55.70	52.60	29.80
5:48	2.46	-0.18	0.18	-0.87	-21.20	27.25	-13.70	-0.50	25.40	82.60	55.90	54.10	28.40
15:49	5.60	-0.40	0.34	-	-53.40	25.00	-14.00	-0.56	23.20	79.30	54.90	53.80	25.60
16:54	4.77	-0.34	0.50	-1.30	-54.20	25.00	-14.00	-0.56	23.20	79.30	54.90	53.80	25.60
17:18	4.43	-0.30	0.17	-	-38.40	25.00	-14.80	-0.59	23.40	79.40	55.00	53.90	25.50
19:48	2.43	-0.11	0.17	0.98	-26.50	25.00	-22.00	-0.88	23.90	79.70	55.00	54.20	25.60
22:33	3.02	-0.09	0.20	0.10	-27.80	26.00	-33.50	-1.29	25.30	81.40	55.60	55.30	26.10
23:46	3.47	-0.15	0.26	0.09	-37.40	25.00	-23.10	-0.93	23.80	79.60	55.40	54.30	25.70
25:00	6.65	-0.23	0.33	0.22	-75.60	29.00	-29.00	-1.00	28.00	85.70	57.00	56.20	29.50
26:59	0.75	0.13	-0.17	0.54	-30.80	25.50	5.80	-0.23	-29.60	53.50	41.70	Imag	Imag
27:27	2.77	-0.18	-0.39	1.05	-75.80	28.00	-15.40	-0.55	16.20	83.60	56.30	54.50	29.10
27:35	1.24	-0.19	-0.27	0.61	-48.30	28.00	-6.50	-0.23	23.90	82.70	55.70	53.10	29.50
27:54	0.79	0.13	-0.17	0.50	-29.40	31.00	6.10	-0.20	-35.50	56.10	41.60	Imag	Imag

Analysis of main sub-pulse for all body-potential surges of Subject 70, Session 7.

7e tells us that F must be negative. Turning to Eq. 6c, we see that this is only possible when:

$$d \sim -\frac{2Y_E}{\sin\theta} \tag{8}$$

Using Eqs. 7c, 7d and 1, we find that:

$$V_U \left[ \frac{\frac{1}{L - Y^*} - \frac{1}{L - 2Y_U + Y^*}}{\frac{1}{2Y_U - Y^*} - \frac{1}{Y^*}} \right] \tag{9a}$$

This is a quadratic equation in  $Y_U$  with the solution:

$$Y_U = \frac{a}{2} \pm \left[ \left( \frac{a}{2} \right)^2 - b \right]^{1/2} \tag{9b}$$

where,

$$a = \frac{1}{2} \left[ (L + 2Y^*) + \frac{(\beta + 1)}{\gamma} \right] \tag{9c}$$

$$b = \frac{Y^*}{4} \left[ \frac{(1 + \beta)}{\gamma} + (2L + Y^*) \right] \tag{9d}$$

and

$$\gamma = \frac{\beta}{Y^*} - \frac{1}{L - Y^*}; \quad (9e)$$

$$\beta = \frac{V_D}{V_U} \quad (9f)$$

Values of  $Y^*$ ,  $\beta$ ,  $\gamma$ ,  $a$  and  $b/Y^*$  are also given in Table 5 along with the calculated values of  $Y_1$  and  $Y_2$ . We note that  $Y_1$  is the only acceptable solution since  $Y_{U2}$  is slightly greater than  $Y^*$  and this would not also allow the required  $V_b/V_D$  values. We note also that thirteen of the fifteen values of  $Y_1$  are mathematically real with almost the same value,  $Y_1 = 54''$ . The other two values are mathematically imaginary and correspond to the two special cases where  $V_1$  and  $V_D$  have the same sign, which is impossible for a single dipole. This result implies that, for these two cases (time = 26:59 and 27:54), a second dipole developed in the head with its negative charge close to the ear and its positive charge closer to the top wall. Since our analysis applies only to the case of a single dipole, these two values of  $Y_{U1}$  must be excluded from the analysis. Although an analysis can be developed for two simultaneous dipole events, there are too many unknowns compared to the presently available data to solve for the origin and characteristics of this second dipole.

Inserting the  $Y_1$  values from Table 5 into Eq. 7d, one can evaluate  $Q$  for each of these cases. In particular, for the  $t = 3:20$  event,  $Q = 6.5 \times 10^{-11}$  coulombs or a charge of only  $4 \times 10^8$  electrons. Thus, for all the events listed in Table 5,  $Q \cong 10^8$  to  $10^9$  electronic charges. This is equivalent to the passage of only  $\sim 0.1$  nanoampere of electric current for  $\sim 1$  second. Precise values for  $(X_F, \theta)$  can be obtained using the value of  $Q$  and Eqs. 7a, 7b for  $V_F$  and  $V_B$ , respectively. However, because of the  $(a, \&)$  effects discussed in the next section, there doesn't seem to be much point in obtaining precise values for each case at the present level of approximation. Finally, as can be seen from Eq. 8,  $d$  is  $\sim 1.5$  to 2 meters since  $\sin\theta \sim -1$ . Thus, the more accurate equation set (Eqs. 7) lead to very similar conclusions to those found using the approximate ( $d/l \ll 1$ ) equation set.

### Illustrating the Importance of $a$ and $\epsilon'$

Three experiments were designed to illustrate the importance of  $a$  and  $\epsilon'$  in the copper-wall study. In advance, though, a 2'' diameter metal sphere was located along the center line of the front and back walls. An abrupt voltage pulse of +35 V was placed on the ball and time-varying  $V_F$ ,  $V_B$ ,  $V_1$  and  $V_D$  recorded for five different vertical positions of the ball. The electrical capacitance of the ball was 20 picofarads. In all cases, wall-voltage recordings were very noisy, though no one was in the copper wall room.

### Experiment 1

To increase capacitance and diminish the electrical noise, a galvanized steel bucket with a capacitance of 160 picofarads was used in place of the metal sphere. The bucket was 13" in diameter at the top and 11.5" in diameter at the bottom with a depth of 10". These capacitance measurements were made between the bucket and ground using the standard impedance bridge technique which gives the capacitance of a human body to be  $\sim 300$  pF to 400 pF. A typical set of voltage recordings is shown in Figs. 5a and 5b for the case where the bucket is almost central in the room (4" closer to the bottom wall). In Fig. 5a, we note that  $V_F$  and  $V_B$  are almost identical (when the 0.02 V offsets are removed) but that the initial magnitude of the wall voltage decreases as the rate of rise of the bucket voltage decreases. Also, the magnitude of the wall voltage falls off with duration of the bucket voltage. This is exactly what one would expect from opposite-sign ion condensation from the air onto the walls. Thus  $a, \ll 1$  ( $a, \sim 10^{-3}$  by calculation to match the  $V_{\text{Wall}} / V_{\text{Bucket}}$  data). In Fig. 5b, similar behavior is seen for  $V_U$  and  $V_D$ . By considering all the data in this experiment, we find that  $1 < a, < 1.5$  for  $V_U$  when  $47.5" > d > 21.5"$ , respectively, and  $1 > a, > 0.7$  for  $V_D$  where  $48" < d < 64"$ , respectively.

### Experiment 2

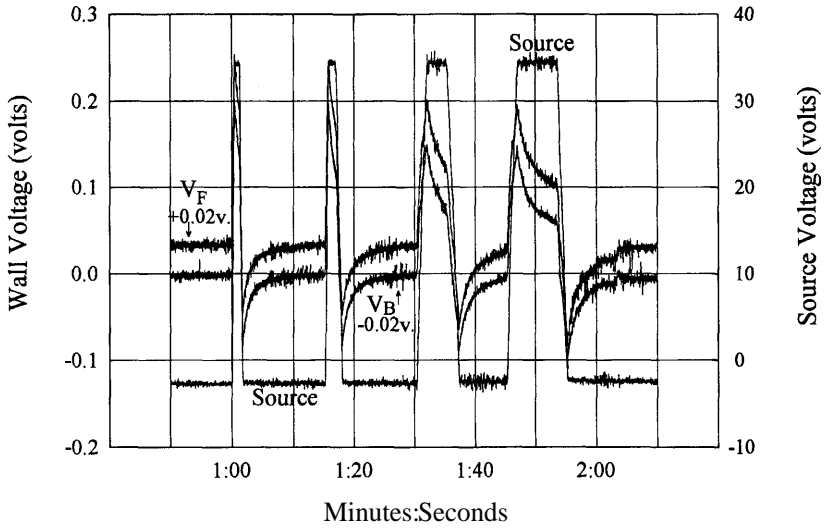
A person stood about 2" behind the bucket, between the bucket and the back wall. For the same position of the bucket as in Fig. 5, Fig. 6 shows the changes associated with the interaction of the bucket charge with the general capacitive properties of the human body. Clearly, the  $\epsilon' \neq 1$  effect is significant and greatly influences the electrodynamic response of the system.

### Experiment 3

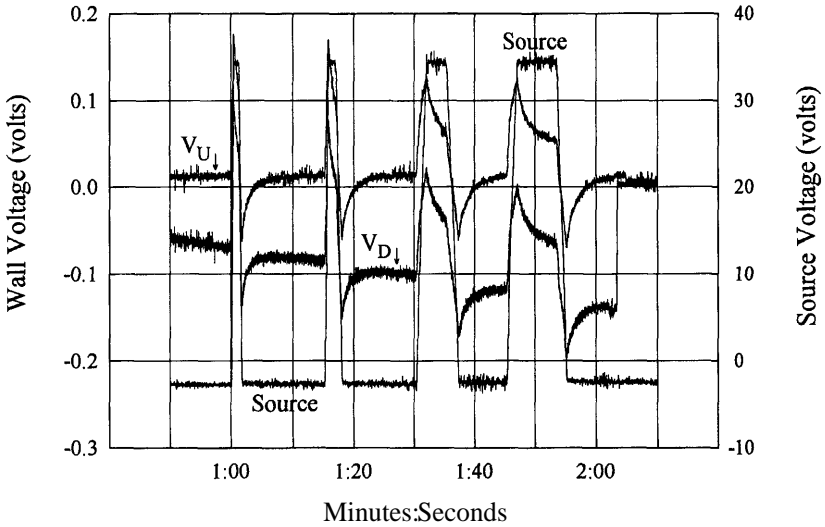
The bucket was removed and a person stood in the center of the copper wall room with an electrode applied to the left ear. When source pulses of 35 V were applied, the wall-voltage responses were those shown in Fig. 7. We note first that these responses are not as electrically noisy as those seen in Fig. 6. However, we also note that  $V_D$  has an appreciably larger magnitude than  $V_U$  even though the distance from the ear electrode to the top wall is only  $\sim 1/5$  the distance to the bottom wall. Interestingly enough, the distance from the top of the head to the top wall is about twice that from the feet to the bottom wall.

## Discussion

In Table 5, we find several instances where  $V_F$  and  $V_B$  have the same sign (at time = 19:48, 22:33, 23:46 and 25:00) and one wonders at the reason for this. By considering Table 3 we see that, for the 19:48 and 22:33 pulses, the therapist was standing and facing  $270^\circ$  (west). For the 23:46 and 25:00 pulses, the therapist was standing and largely facing  $315^\circ$  (north-west). Since the dipole

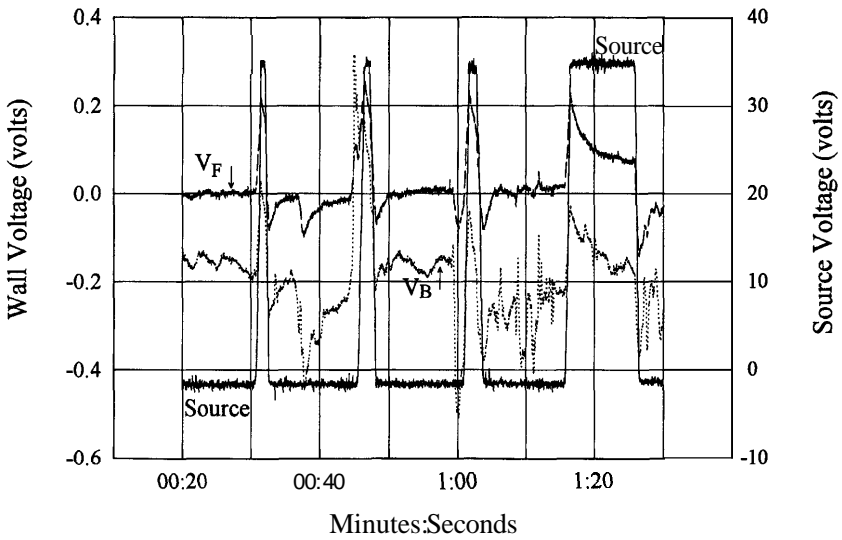


(5a)

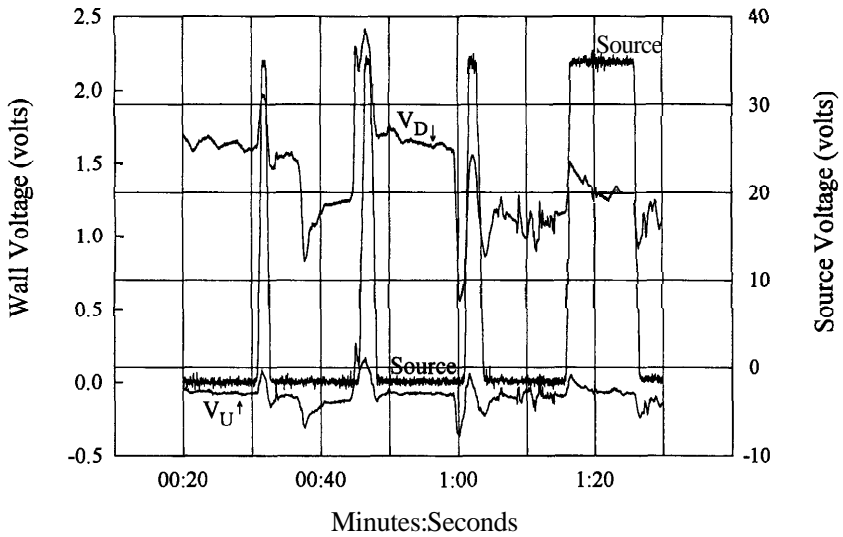


(5b)

Figs 5a and 5b. Typical set of simultaneous voltage recordings on a deliberately charged metal bucket and the four copper walls (no human in the room; bucket almost central in the room (4" closer to bottom wall)). The four wall voltages,  $V_F$ ,  $V_B$ ,  $V_U$  and  $V_D$ , are shown in 2 graphs to avoid visual confusion. In addition,  $V_F$  and  $V_B$  are displaced by addition or subtraction of 0.02 V to enhance visibility.

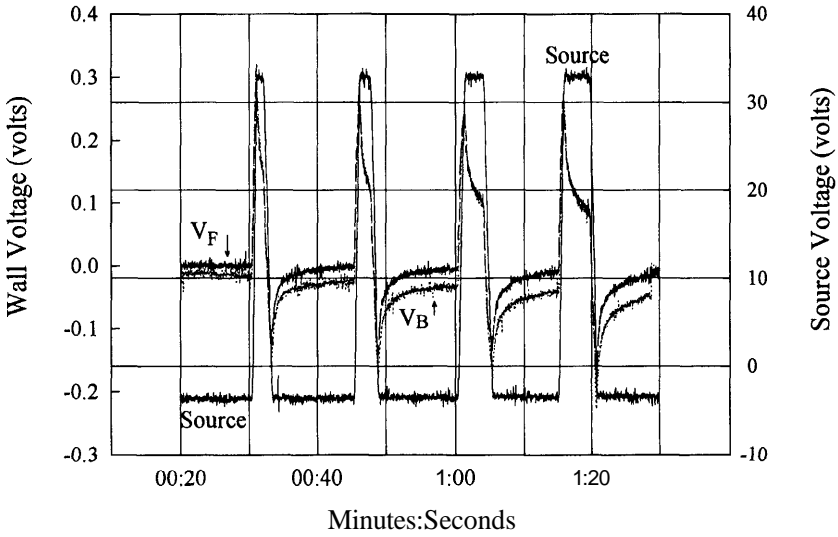


(6a)

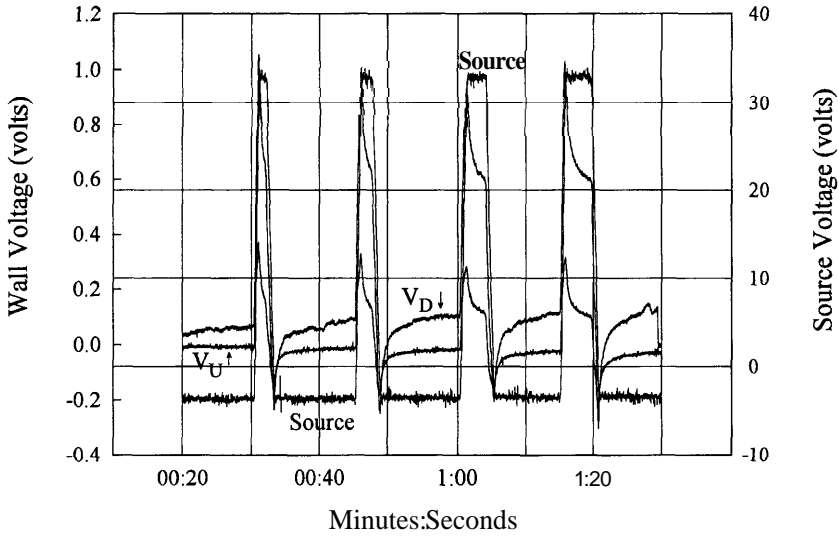


(6b)

Figs 6a and 6b. Simultaneous voltage recordings on a deliberately charged metal bucket and the four copper walls (bucket almost central in the room, 4" closer to bottom wall); human standing about 2" behind the bucket (closer to back wall).



(7a)



(7b)

Figs 7a and 7b. Simultaneous voltage recordings on a deliberately charged right ear (of a human standing centrally between the front and back copper walls) and the four copper walls.

is from the ears to the feet, if the negative-charge centroid is aligned vertically over the positive-charge centroid, essentially no voltage should appear on the front and back walls except for slight differences in the  $a$ , and  $a$ , effects for these walls. The relevant point here is the differentiation between a sitting and a standing therapist.

In Table 5, the pulses at 26:59 and 27:54 indicate that  $V_U$  and  $V_D$  have the same sign of voltage. Is this due to a second dipole in the head as mentioned earlier or is this also due to some artifact of body orientation or movement? In both cases the therapist is standing and some small head and body motion exists, but it is not immediately apparent how movement of the negative charge end of the dipole can influence the sign of the upper wall voltage. Perhaps the  $a$ , and  $a$ , effects are playing a role here as well. Since the combined magnitude of these two effects is so large, their involvement cannot be ruled out by the present experiments.

We found from Table 5 that  $Y_D = 31''$  when the therapist was sitting or standing while  $d = 54''$  to  $60''$ . We might speculate that the origin of the dipole formation is the oriental "Dan Tian" (or "Hara") subtle-energy point, located approximately three fingers' breadth below the navel; however, a more precise analysis will be needed to verify this specific site involvement. Although the hypothesized kidney meridian starts on the sole of the foot (K1) and proceeds up the leg to the back of the knee (K10) and then reappears in the lower abdomen (K11) to travel up the front center line of the body and end at the clavicle (K27), an energetic connection between K27 and the ears would complete the ear-abdomen-foot dipole. One question needing an answer in future studies is: "Does the net-charge difference manifest only at the ends of the dipole or is it distributed along the path from  $(X_F, Y_D)$  to the ears and the feet?" The mechanism of charge transfer during dipole formation and collapse would depend critically on the answer to this question.

Polarization response of the body's internal dielectric structure paralleling the time-dependent body-electrolyte charge displacement, plus opposite sign ion condensation onto the copper walls from the air, constitute the main dynamical aspects of the experimental data.

Lastly, what rationale can be given for the creation of the dipole causing the voltage pulse? We propose the following working hypothesis: In some as-yet-unknown way, the subject's intentionality imposes a force on a subtle-energy structure of the body (Tiller, 1993), leading to the transmission of subtle radiations, which, for identification purposes only, shall be labeled  $\Delta\chi(t)$  (see Fig. 8). Transduction effects are thought to occur because of coupling between this subtle-body structure and the subject's physical-body structure, creating a pulse of magnetic vector potential,  $\Delta\mathbf{A}(t)$ , at some location in the physical body where

$$\Delta\mathbf{A}(t) = \mathbf{f}(\Delta\chi(t)) \quad (10)$$

where  $\mathbf{f}$  stands for a functional relationship between  $\mathbf{AA}$  and  $\Delta\chi$ . One of us

(Tiller, 1993) has proposed that  $\mathbf{A}$  is the bridge between the hypothesized sub-*tle*-energy domain and the dense physical domain of physics and chemistry.

Given a local pulse,  $\Delta\mathbf{A}(t)$ , conventional electrodynamics (Kraus, 1973) yields pulses of local electric field,  $\Delta\mathbf{E}(t)$ , and magnetic field,  $\Delta\mathbf{B}(t)$ , given by:

$$\Delta\mathbf{E}(t) = \frac{-\partial\Delta\mathbf{A}(t)}{\partial t} \quad (11a)$$

$$\Delta\mathbf{B}(t) = \nabla \times \Delta\mathbf{A}(t) \quad (11b)$$

The time correlation of  $\Delta\chi$ ,  $\Delta\mathbf{A}$ , and  $\Delta\mathbf{E}$  are thought to be as illustrated schematically in Figure 8. Given such a pulse of electric field as described by Equation 11a, a force exists for charge separation of the body electrolytes at that particular body location which is the origin of  $V_b(t)$ .

To resolve some of these critical issues, it would be useful to modify the experimental system as follows: (a) add some high frequency magnetic-field detectors to the instrumentation in order to provide independent determination of  $\Delta\mathbf{A}(t)$  via Eq. 11b, (b) add independent, electrically isolated, microelectrodes (Langmuir probes) at the center of each wall in order to have voltage readings that minimize the opposite-ion condensation effect and (c) add additional electrodes at other body locations in order to evaluate the spatial aspects of the dynamic dielectric body response to the initial dipole. Present plans for replication of this research include further tests with the 9 healers already studied, but instrumented with four body electrodes (ear, ankle, abdomen and back) instead of ear only.

Although data for  $X_f$  at the dipole source could have been readily calculated, to see if the location of the dipole source was always in the front, center or rear portion of the abdomen, the uncertainties in  $Y_{Uf}$  and the neglect of the electrodynamic aspects, and the lack of exact information on the tilt of the therapist's body, introduce errors that make such an exercise insufficiently precise to be worth doing. On another front, not all of the Gaussian sub-pulses in the deconvolution profile have been analyzed. The reason: When there are 4 to 10 subpulses in a body-potential surge, the electrodynamic aspects of the problem shifts the centerlines of the wall-voltage sub-pulses relative to those for the body and it becomes almost impossible to pick the proper set of wall sub-pulses that belong to a given body sub-pulse.

## Conclusions

1. The simple charge-dipole model, in the electrostatic limit, seems to qualitatively represent the voltage pulse data from TT therapists in the Copper Wall Study (Green et al., 1991).

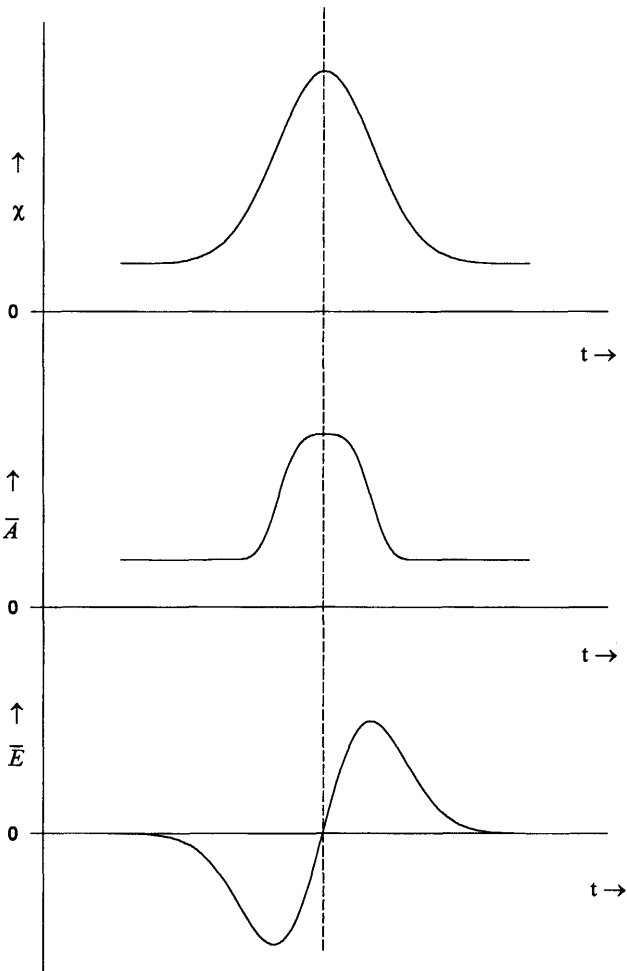


Fig. 8. Schematic illustration of a subtle energy pulse,  $\chi$ , generating a magnetic vector potential pulse,  $A$ , which, in turn, generates an electric field,  $E$ .

2. The primary dipole origin is in the region of the lower abdomen with the charge-separation length being approximately from head to foot, with the head region manifesting the negative charge.
3. Opposite-sign ion collection on the copper walls significantly influences the quantitative conclusions of this study. Neglecting this factor,  $\sim 10^8$  to  $10^9$  unit electronic charges appear to be transferred during dipole formation.

4. Dynamic dielectric polarizations of various body parts appreciably perturb the quantitative aspects of the simple electric-dipole response model.
5. Multiple charge-image effects in the copper walls are present but influence the results only within a factor of two.
6. The details of the wall-voltage data differ depending upon whether the TT therapist is standing or sitting, and upon the body's rotational orientation with respect to the walls.

### Acknowledgments

We are grateful for support from the three members of the Rockefeller Office of Philanthropy, New York, and Fred Matser, Netherlands.

### References

- Green, E. E., Parks, P., Guyer, P., Fahrion, S., and Coyne, L. (1991). Anomalous electrostatic phenomena in exceptional subjects. *Subtle Energies*, 2, #3, 69.<sup>2</sup>
- Krieger, Dolores. (1995). Personal communication to Elmer Green [March 1995].<sup>3</sup>
- Kraus, J. D. and Carver, K. R. (1973). *Electromagnetics*. McGraw-Hill Book Company, New York.
- Tiller, W. A. (1993). What are subtle energies? *Journal of Scientific Exploration*, 7, 293.

---

<sup>2</sup>The nine healers who participated in the Copper Wall Project were referred to generically as "Non Contact Therapeutic Touch therapists." In the present paper, the semantically-misleading modifier, "non-contact," is not used.

<sup>3</sup>In Therapeutic Touch (TT) the word "Touch" refers to the healer's touch on the scientifically-hypothesized "subtle physical body" of the patient. It is not touch on the "dense physical body." The use of the adjectival modifier, "non contact," in the sometimes-used expression, Non Contact Therapeutic Touch, suggests that there are two kinds of Therapeutic Touch. This is incorrect. All certified Therapeutic Touch therapy, as taught and practiced under that name in more than 100 U.S. hospitals, is, and always has been, "non contact." Apologies and thanks to Dolores Krieger, R.N., Ph.D. for clarification of this issue.

When working with patients in the Copper Wall Project, several healers reported that they "felt," tactually (while not physically touching the patient's body), the "surface" of the patient's "subtle energy body." These healers often spoke of a patient's physical dysfunctions in terms of how the "subtle energy body" felt, to them, over a specific part or region of the body, cool or cold, hot or burning, empty or congested, etc., apparently depending on individual interpretation of sensation. An investigation of uniformity among healers in describing tactual contact with a patient's "subtle energy body," using a single well-diagnosed patient, would make an interesting research project. It would answer a few psychological and parapsychological questions, and raise many others.